COMMUN. MATH. SCI.
Vol. 15, No. 2, pp. 555–564


*FAST COMMUNICATION*

# GENERALIZED SHOCKLEY–RAMO THEOREM IN ELECTROLYTES*

PEI LIU†, CHUN LIU‡, AND ZHENLI XU§

**Abstract.** The charge motion in vacuum and the induced currents on the electrodes can be related through the Shockley–Ramo (SR) theorem. In this paper, we develop a generalized Shockley–Ramo (GSR) theorem, which could be used to study the motion of macro charged particles in electrolytes. It could be widely applied to biological and physical environments, such as the voltage-gated ion channels. With the procedure of renormalizing of charge and dipole, the generalized theorem provides a direct relationship between the induced currents and the macro charge velocity. Compared with the original Shockley–Ramo theorem, the generalized Shockley–Ramo theorem avoids integrating all the ionic flux, which could reduce the computational cost significantly.

**Keywords.** Shockley–Ramo theorem, electrolytes, charge renormalization, inverse problem.

**AMS subject classifications.** 35Q70, 82B21, 82C05, 92C30.

## 1. Introduction

Shockley-Ramo theorem [28, 31] presents a relationship between the instantaneous induced current on an electrode and the charge motion in the vicinity. By realizing that the current is induced by the electrostatic flux change on electrodes instead of the amount of electrons arriving or leaving, the theorem considers the total current including the displacement current and the particle current. It can be viewed as an extension of Kirchhoff's law. Shockley–Ramo theorem has received wide applications in semiconductors as well as nuclear devices [12, 18, 24]. Commonly the induced currents can be easily measured by experiments and we can thus infer the charge velocity through the Shockley–Ramo theorem, which is the basic principle of radiation detection techniques.

When applied to systems with lots of charged particles, the theorem requires to sum up the contributions of all charges. It is very expensive to employ Shockley–Ramo theorem to determine the trajectory of a macro charge in the electrolytes, which is also difficult to measure directly in experiments.

One of the most important application is the charged residuals called voltage sensor which contribute to the conformational change under external fields in voltage-gated ion channels [4,13]. The molecular structure of a channel protein has been characterised by crystallography in a frozen state [1, 6, 29]. And the real-time conformational dynamics has been obtained through fluorescence microscopy [34], which is at the subcellular level

*Received: March 29, 2016; accepted (in revised form): August 13, 2016. Communicated by Jie Shen.

The research of P. Liu and Z. Xu is supported by the NSFC (Grant Nos. 91130012 and 11571236), the Chinese Organization Department, and the HPC Center of Shanghai Jiao Tong University. The research of C. Liu is partially supported by NSF (Grant Nos. DMS-141200 and DMS-1216938). The authors also thank Prof. Bob Eisenberg for the valuable discussion and comments. P. Liu and Z. Xu would like to thank the Department of Mathematics of the Penn State University for hosting their visits and providing the great working environment.

†School of Mathematical Sciences, and Institute of Nature Sciences, Shanghai Jiao Tong University, Shanghai 200240, P.R. China (hgliupei1990@sjtu.edu.cn).

‡Department of Mathematics, The Penn State University, University Park 16801, USA (liu@math.psu.edu).

§School of Mathematical Sciences, Institute of Nature Sciences, and MoE Key Lab of Scientific and Engineering Computing, Shanghai Jiao Tong University, Shanghai 200240, P.R. China (xuzl@sjtu.edu.cn).

and not valid for intracellular sites. Or by using a special-designed computer for high-speed molecular dynamic simulation, Jensen et al. [16] reported the gating mechanism in a potassium channel, which is still considered too expensive for a wide application.

Since direct measurements remains unsatisfactory, indirect methods mainly rely on the measurement of the electrical signals, especially the induced currents [3, 17, 30] in voltage-clamp or patch-clamp [23] experiments. Continuum models has been often used to quantitatively understand the behaviour of electrolytes. The kinetic properties of ion transport could be described by Poisson–Nernst–Planck (PNP) equations with density functional theory or field theoretical models [7, 9, 11, 14, 20, 32, 35] or by using an energetic variational approach [8, 15] to properly take into account the electrostatic and hard core correlations. All these PNP-type models are solving a forward problem: given the charged particle velocity, we aim to solve the gating current. However, in real experiments, the quantity being measured is the gating current, thus we need to formulate an inverse problem [5] to reconstruct the particle trajectory. It is generally considered to be too expensive to solve this inverse problem.

Compared to small ions, voltage sensor which is actually composed of amino acids, can be considered as a macro particle. And we are only interested in the trajectory of the voltage sensor instead of how the ions move. For the purpose, we generalize the Shockley–Ramo theorem to systems in electrolytes, which can be used directly for understanding the macro charged particle motion in electrolytes. The generalized Shockley–Ramo theorem gives a simple relation between macro particle velocity and the induced currents, avoiding the integration of all the electrolyte flux. With this theorem, it will be much more convenient to solve the inverse problem without much computational cost. As an important application, it could help us understand the ion channel property and the gating dynamics quantitatively.

## 2. Mathematical model and methods

The induced current and charged particle velocity in electrolytes are related. In this section, we will use the ion channel problem as an example to illustrate the generalized Shockley–Ramo (GSR) theorem. We want to figure out how the charged residual move with the current measured.

**2.1. Ion channel model.** The ion channel model is schematically shown in Figure 2.1. The electrolytes represent the intra- and extracellular fluids, respectively. The technique developed in [27, 33] abolishing the ionic conduction allows us to block the channel so that no ion can move from one side to another. The labeled voltage sensor can receive external stimulus and move. Two electrodes are grounded, where the induced currents are measured. Electron cannot transfer from electrode to electrolyte, or vice versa.

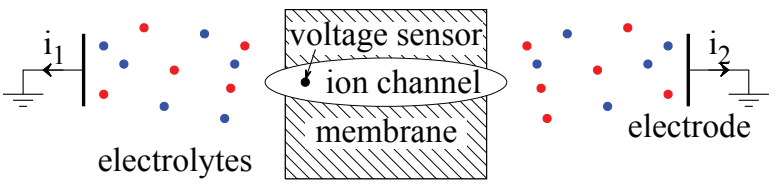


FIG. 2.1. *Schematic diagram of a voltage gated ion channel. The amino acid's motion can determine the state of channel: open or closed. We use* $\Omega$ *to represent the domain of electrolyte and* $B$ *for ion channel,* $\Gamma_1$ *for left electrode and* $\Gamma_2$ *for right electrode. The detailed structure of ion channel protein is not shown in the diagram.*

The governing equation for the forward problem could be written as

$$\begin{cases} -\nabla\cdot\epsilon\nabla u = \sum_k z_k c_k(\mathbf{r}) & \text{in } \Omega, \\ -\nabla\cdot\epsilon\nabla u = q\delta(\mathbf{r}-\mathbf{s}(t)) & \text{in } B, \\ \dfrac{d}{dt}c_k + \nabla\cdot J_k = 0 & \text{in } \Omega, \end{cases} \tag{2.1}$$

where $\mathbf{s}(t)$ is the position of the amino acid at time $t$ which takes charge $q$, $\epsilon$ is the dielectric permittivity, $\epsilon = \epsilon_w$ in $\Omega$ and $\epsilon_0$ in $B$. $c_k$ and $z_k$ are ion density and valence of $k$th ionic species, respectively, and $J_k$ is the flux, whose exact form depends on the model we use. The interface conditions for the electrical potential $u$ are the continuities of $u$ and its normal derivative $\epsilon\partial u/\partial\vec{n}$. A mean-field theory gives the fluxes of the PNP equations: $J_k = -D_k(\nabla c_k + c_k\nabla u)$, with $D_k$ being the diffusion coefficient. The surface charge density at electrodes are represented by: $\sigma_\alpha = -\partial u/\partial\vec{n}|_{\Gamma_\alpha}$, where $\alpha = 1$ or 2, corresponding to the left or right electrode, respectively, $\vec{n}$ is the outer normal direction. Induced currents per area are thus: $i_\alpha = -\partial\sigma_\alpha/\partial t$.

We have now built up the relationship to compute the induced currents from given charge trajectory. By solving the inverse problem, we could be able to understand the transport of charged particles, such as the gating mechanism in ion channel problem. However, due to the high dimensions and highly nonlinearity of the forward problem, the corresponding inverse problem requires to solve the forward problem many times, and is thus very time consuming.

**2.2. Shockley–Ramo theorem and its generalization.** The original Shockley–Ramo (SR) theorem is derived in vacuum area $D$, while neglecting the magnetic and radiation effects. Consider the moving particle with grounded electrodes where electrical signals are measured. The equation for electric potential is the following Poisson equation:

$$\begin{cases} -\nabla\cdot\epsilon\nabla\phi = q\delta(\mathbf{r}-\mathbf{s}(t)) & \text{in } D, \\ \phi|_{\partial D} = 0, \end{cases} \tag{2.2}$$

where $\phi$ is electrical potential, $q$ and $\mathbf{s}(t)$ are the charge and instantaneous position of the moving particle, and $\partial D$ is the boundary consisting of all electrodes.

We introduce another potential, which describes the intrinsic information of the system, satisfying the following:

$$\begin{cases} -\nabla\cdot\epsilon\nabla\psi = 0 \text{ in } D, \\ \psi|_{\partial D\setminus\Gamma} = 0, \\ \psi|_\Gamma = 1, \end{cases} \tag{2.3}$$

where $\Gamma$ is one of the the electrode surfaces. By means of Green's identity, we have

$$\int_D (\phi\nabla\cdot\epsilon\nabla\psi - \psi\nabla\cdot\epsilon\nabla\phi)\,dx = \int_{\partial D} \epsilon\left(\phi\frac{\partial\psi}{\partial\vec{n}} - \psi\frac{\partial\phi}{\partial\vec{n}}\right)dS. \tag{2.4}$$

By using Equations (2.2) and (2.3), the left-hand side reduces to, $q\psi(\mathbf{s}(t))$, and the right-hand side becomes,

$$-\int_\Gamma \epsilon\frac{\partial\phi}{\partial\vec{n}}dS = q_{\text{ind}}, \tag{2.5}$$

where $q_{\text{ind}}$ is the induced charge on the electrode surface. Finally, by taking the time derivative on both sides, we arrive at the SR theorem, which states,

$$i \triangleq -\frac{d}{dt} q_{\text{ind}} = q\vec{v} \cdot \vec{E}, \tag{2.6}$$

where $i$ is the current induced by the particle motion, $\vec{v}$ is its velocity, $\vec{E}$ is the electrical field at the particle's instantaneous position.

The SR theorem has been generalized to many cases, for example, time-dependent dielectric media [26] and electrodynamic simulation [36, 37]. It is suggested that the gating particle motion induced current could be represented through the SR theorem [10, 25], which requires the knowledge of all the particle velocity or ionic fluxes to compute the induced current. However, the ionic flux is coupled with the motion of the charged particle in a nonlinear manner, which is the key difficulty in analyzing the gating mechanism. Directly employing the SR theorem might not be efficient, it still needs to solve the inverse transport problem for the conformation change.

Compared to small ions, the motion of amino acids is usually very slow. Thus it is reasonable to assume the system to be at the quasiequilibrium state for all time. This would allow us to write the ionic distribution as a function of the electrical potential and use equilibrium theory to study the charged system. Note that the electrode surface charge density as well as the induced currents are only related with the local property of electrical potential. For equilibrium system, the far field behavior (near bulk) could be described by using linearized PB equation, with renormalized boundary/interface conditions [2,19]. More detail will be presented in the next subsection. So, the electrical potential $u$ at time $t$ could be represented by

$$\begin{cases} -\nabla^2 u + \kappa^2 u = 0 & \text{in } \Omega, \\ -\nabla \cdot \epsilon \nabla u = (q_r + \vec{p_r} \cdot \nabla)\delta(\mathbf{r}, \mathbf{s}(t)) & \text{in } B, \\ u|_{\partial(\Omega \cup B)} = 0, \end{cases} \tag{2.7}$$

where $\kappa = \sqrt{\frac{\sum_k c_k z_k^2}{k_B T \epsilon_w}}$ is the inverse Debye length, $k_B$ is the Boltzmann constant and $T$ is the temperature. $q_r$ is the renormalized charge, and $p_r$ is the renormalized dipole due to the geometry asymmetry. Also, we might need to introduce quadrupole and even multipole expansion for more accurate description of a complex geometry. We shall require the electrodes to be far away from the channel to ensure the far field condition. The electrodes are also assumed to be grounded, so there is no another double layer structure near the electrodes, which cannot be described by the linearized theory.

Now, as in the SR theorem, we introduce intrinsic potentials $\Phi_\alpha$, which will be used to derive induced currents at electrodes,

$$\begin{cases} -\nabla^2 \Phi_\alpha + \kappa^2 \Phi_\alpha = 0 & \text{in } \Omega, \\ -\nabla^2 \Phi_\alpha = 0 & \text{in } B, \\ \Phi_\alpha|_{\partial(\Omega \cup B) \setminus \Gamma_\alpha} = 0, \\ \Phi_\alpha|_{\Gamma_\alpha} = 1, \end{cases} \tag{2.8}$$

where $\alpha = 1$ or 2, indicating left or right electrode. By means of Green's identity, we get,

$$\int_{\Omega \cup B} (u\nabla \cdot (\epsilon \nabla \Phi_\alpha) - \Phi_\alpha \nabla \cdot (\epsilon \nabla u))\, dx = \int_{\partial(\Omega \cup B)} \epsilon \left( u \frac{\partial \Phi_\alpha}{\partial \vec{n}} - \Phi_\alpha \frac{\partial u}{\partial \vec{n}} \right) dS, \tag{2.9}$$

the surface charge is, thus,

$$\sigma_\alpha = q_r\Phi_\alpha - \vec{p}_r\cdot\nabla\Phi_\alpha = q_r\Phi_\alpha + \vec{p}_r\cdot\vec{E}_\alpha; \tag{2.10}$$

the induced current is

$$i_\alpha = \left(q_r\vec{E}_\alpha - \Phi_\alpha\nabla q_r + \nabla(\vec{p}_r\cdot\vec{E}_\alpha)\right)\cdot\vec{v}. \tag{2.11}$$

This is the GSR theorem. And for the cases where higher order renormalized multipoles are needed, the extension is straight forward.

**2.3. Charge renormalization.** The charge renormalization has been widely used in colloidal sciences [2]. It is originally applied to solve the nonlinear PB equation, though it can be used for a general system where the nonlinear PB equation fails, which states that the electric potential at the far field can be the solution of linearized equation but with a renormalized surface charge. The charge renormalization is also known as Manning counterion condensation in polyelectrolytes [21, 22].

In literature [19], only a renormalized charge has been discussed in colloidal applications, and the renormalized multipoles are usually ignored. In our problem, we should additionally introduce the renormalized dipole, which can be significantly important. To understand this, let us consider a simple example: the PB equation in one dimension, for which the renormalized charge and dipole could be computed analytically, as

$$\begin{cases} u_{xx} = \kappa^2\sinh u & \text{for } x < -x_1, \\ -\varepsilon u_{xx} = q\delta(x) & \text{for } -x_1 < x < x_2, \\ u_{xx} = \kappa^2\sinh u & \text{for } x > x_2, \end{cases} \tag{2.12}$$

where $\varepsilon = \epsilon_0/\epsilon_w$ is the ratio of dielectric constants between vacuum and water.

The solution of the system (2.12) for $x < -x_1$ and $x > x_2$ and corresponding far field $|x| \to \infty$ asymptotic leading term are given by,

$$\begin{cases} u_1 = 2\log\dfrac{1+C_1e^{\kappa(x+x_1)}}{1-C_1e^{\kappa(x+x_1)}} \sim 4C_1e^{\kappa(x+x_1)}, \\ u_2 = 2\log\dfrac{1+C_2e^{\kappa(x_2-x)}}{1-C_2e^{\kappa(x_2-x)}} \sim 4C_2e^{\kappa(x_2-x)}, \end{cases} \tag{2.13}$$

where $C_1$ and $C_2$ are constants to be determined. And the solution in $-x_1 < x < x_2$ is a continuous piecewise linear function with a jump of the electrical displacement at $x = 0$. By continuous conditions of the potential and electrical displacement at $x = -x_1$ and $x_2$, we have

$$\begin{cases} 2\log\dfrac{1+C_1}{1-C_1} + \dfrac{4C_1\kappa}{1-C_1^2}\dfrac{x_1}{\varepsilon} = 2\log\dfrac{1+C_2}{1-C_2} + \dfrac{4C_2\kappa}{1-C_2^2}\dfrac{x_2}{\varepsilon}, \\ \dfrac{4C_1\kappa}{1-C_1^2} + \dfrac{4C_2\kappa}{1-C_2^2} = q. \end{cases} \tag{2.14}$$

This set of equations give a unique physical solution of $(C_1, C_2)$ for different $(x_1, x_2)$. The asymptotic behaviors at far field can be viewed as the solution of the following linearized PB equation,

$$\begin{cases} -u_{xx} + \kappa^2 u = 0 & \text{for } x < -x_1, \\ -\varepsilon u_{xx} = q_r\delta(x) + p_r\delta_x(x) & \text{for } -x_1 < x < x_2, \\ -u_{xx} + \kappa^2 u = 0 & \text{for } x > x_2, \end{cases} \tag{2.15}$$

where

$$\begin{cases} q_r = 4\kappa(C_1 + C_2), \\ p_r = 4C_1(\varepsilon + \kappa x_1) - 4C_2(\varepsilon + \kappa x_2). \end{cases} \tag{2.16}$$

Equation (2.15) could be written into other forms, for example without the interfaces: $x_1$ and $x_2$. The corresponding equation, Equation (2.16), should also be different. For general 3D cases, the renormalized charge and dipole or even higher order multipole expansion can be fitted through nonlinear PDEs, Monte Carlo, or molecular dynamics simulations. Since this is the equilibrium problem instead of a dynamic one, the computational cost for such simulations to determine the renormalized quantities would be relatively cheap. For a given ion channel, we only need to perform simulations to record renormalized charges and dipoles at several nodes, then we can use these information directly with the help of the GSR theorem to predict the property of the conformation change.

## 3. Numerical results and discussion

To validate the effectiveness of the GSR theorem, we perform numerical computations with the analytically computed renormalized charge and dipole, and compare the results with the direct numerical solution of the PNP equations. The PNP equations are solved by using a finite difference method which has second order accuracy in both time and space discretizations.

We assume the electrolytes on both sides consist of two ionic species of valence $z = \pm 1$ and bulk concentration $c_b = 100mM$. The electrolyte fluxes follow the PNP equations, whose stationary state can be described by the PB equation. At $t = 0$, the system is at equilibrium. Then the charged particle gains a constant velocity $\dot{s}(t) = v$, and the electrolyte starts to flow in response,

$$\begin{cases} \dfrac{d}{dt}c_k = \dfrac{d}{dx}\left(\dfrac{d}{dx}c_k + c_k\dfrac{d}{dx}u\right), \\ -\dfrac{d}{dx}\epsilon\dfrac{d}{dx}u = \displaystyle\sum_k c_k z_k + q\delta(x - s(t)), \end{cases} \tag{3.1}$$

where $q$ is the surface charge density of the charged particle, $s(t)$ is the charged particle's position at time $t$. We assume a fixed voltage and concentration for the boundary conditions at $\Gamma$. The interface condition at the membrane boundary is the electrical potential and electrical displacement continuities, and the ionic flux in channel area is zero since the channel is blocked. The surface charge on the electrodes could be represented by $\sigma_1 = -du/dx|_{\Gamma_1}$ and $\sigma_2 = du/dx|_{\Gamma_2}$. Due to the planar geometry, the GSR theorem gives,

$$\begin{cases} i_1 = \left(q_r E_1 - \Phi_1\dfrac{d}{dx}q_r + E_1\dfrac{d}{dx}p_r\right)v, \\ \\ i_2 = \left(q_r E_2 - \Phi_2\dfrac{d}{dx}q_r - E_2\dfrac{d}{dx}p_r\right)v, \end{cases} \tag{3.2}$$

for which the renormalized charge and dipole as functions of $s(t)$ are shown in Figure 3.1.

The performance of the GSR theorem with respect to different surface charge densities $q$ are shown in Figure 3.2. For low $q$, the renormalized $p_r$ is small and negligible

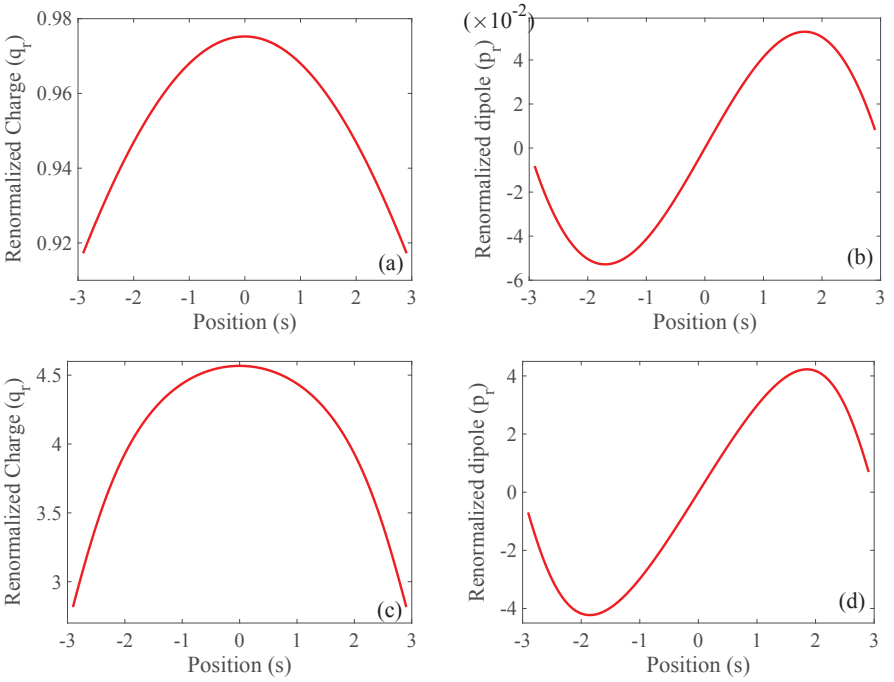


FIG. 3.1. *Renormalized charge and dipole for one dimensional ion channel. (a) and (b): $q=1$; (c) and (d): $q=10$.*

(Figure 3.1). In the case of high $q$, however, $p_r$ is comparable with $q_r$ and its influence becomes significant. The large difference at small $t$ comes from the relaxation of the PNP equation. Within the relaxation time period from the beginning, the quasiequilibrium assumption is not valid. After that, the behaviors of the induced currents from the PNP equations and using GSR theorem tend to be the same. We can also observe that, when the surface charge density is low, $q_r \approx q$ and $p_r \approx 0$, there would not be much error if we use SR theorem directly without the charge renormalization, while for a high $q$, the charge renormalization is essential. At very large $q$, the prediction using the GSR theorem deviates from the correct value, but it maintains well the behavior of the induced current. This deviation is understandable, mainly comes from the system perturbation from the equilibrium state increases with the particle charge. The velocity of the charged particle is also relevant to the validity of GSR theorem, as shown in Figure 3.3. The numerical results are consistent with our analysis that the performance of the GSR prediction works well for small velocity of the charged particle.

At last, the charge renormalization is used in near bulk region, which requires the distance from the channel to the electrode to be large. However, when the distance is larger, the measured electric signal becomes weaker and will be drown in the noise. We show these numerical results in Figure 3.4.

## 4. Conclusion

We have derived a GSR theorem which is useful for predicting the charge motion in electrolytes. This theorem allows us to compute the motion of one macro-particle from the induced current without integrating all the ionic flux. The results of this work

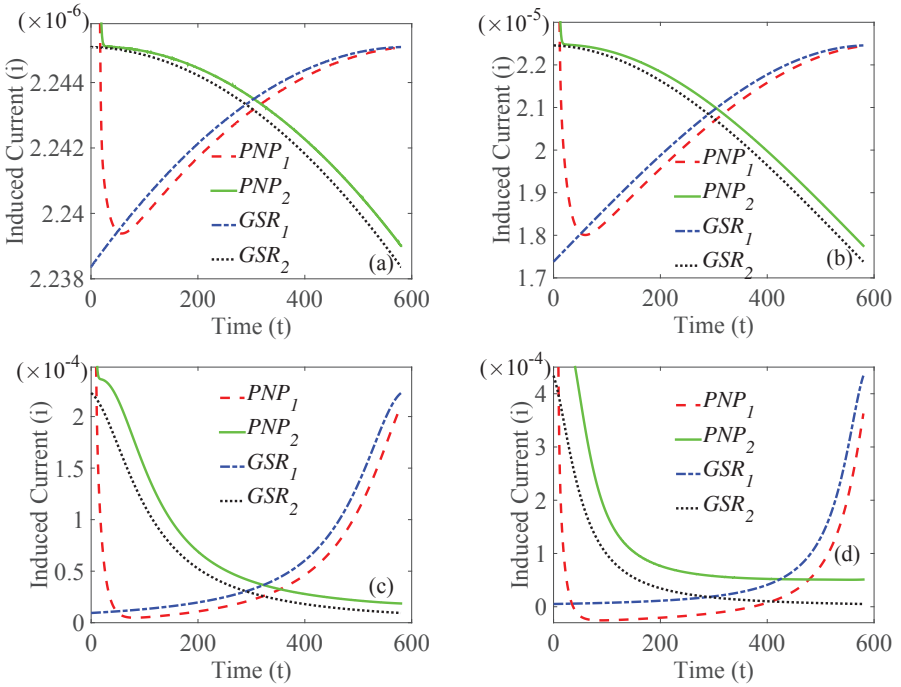


FIG. 3.2. *PNP are computed through solving PNP equation. GSR are from generalized Shockley–Ramo formula* (3.2). *(a):* $q=0.1$, *(b):* $q=1$, *(c):* $q=10$, *(d):* $q=20$.

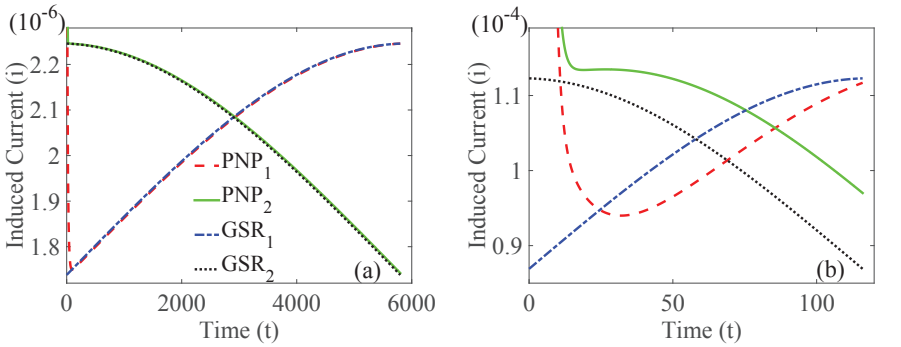


FIG. 3.3. *Induced current for different velocity* $v$. *(a):* $v=0.001$; *(b):* $v=0.05$.

are derived based on the following three conditions: (i) The charged particle movement is slow, compared to the relaxation of electrolytes; (ii) the electrodes should be placed properly such that neither too close nor too far away to the channel, in comparison with the inverse Debye length; and (iii) the electrodes which measure the induced currents should be grounded. Through the procedure of charge and dipole renormalization, the GSR theorem shows a linear relation between the induced current and the charge velocity, where the coefficients can be precomputed through numerical and simulation methods. We can then avoid to solve the inverse problem from the PNP-type equations

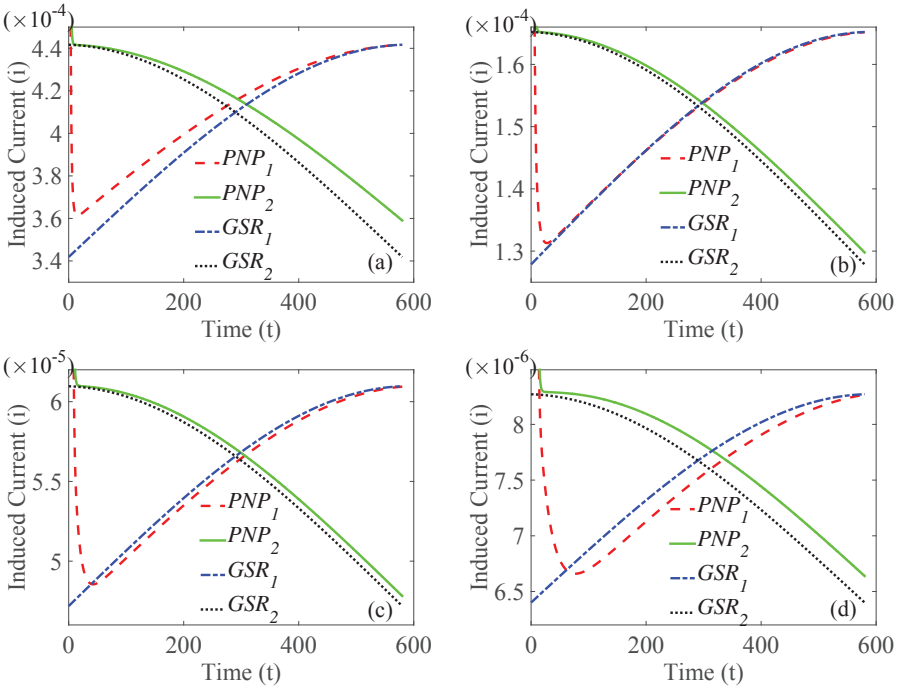


FIG. 3.4. *Induced current for different distances to the electrodes. (a): $L=2/\kappa$; (b): $L=3/\kappa$; (c): $L=4/\kappa$, (d): $L=6/\kappa$.*

to predict the motion of a macro-particle. Also, the complex geometry of the charged particle can be represented through the renormalized multipoles, which allow us to consider real 3-dimensional problems. Since the computational cost can be reduced dramatically, the GSR theorem is useful in understanding the induced currents in many fields, including the gating dynamics in voltage-gated ion channels.

## REFERENCES

[1] A. Abbott, *Ion channel structures: They said it couldn't be done*, Nature, 418:268–269, 2002.
[2] S. Alexander, P. Chaikin, P. Grant, G. Morales, P. Pincus, and D. Hone, *Charge renormailzation, osmotic pressure, and bulk modulus of colloidal crystals: Theory*, J. Chem. Phys., 80:5776–5781, 1984.
[3] C.M. Armstrong and F. Bezanilla, *Currents related to movement of the gating particles of the sodium channels*, Nature, 242:459–461, 1973.
[4] R. Blumenthal, C. Kempf, J. Van Renswoude, J.N. Weinstein, and R.D. Klausner, *Voltage-dependent orientation of membrane proteins*, J. Cell. Biochem., 22:55–67, 1983.
[5] M. Burger, *Inverse problems in ion channel modelling*, Inverse Probl., 27:083001, 2011.
[6] D.A. Doyle, J.M. Cabral, R.A. Pfuetzner, A. Kuo, J.M. Gulbis, S.L. Cohen, B.T. Chait, and R. MacKinnon, *The structure of the potassium channel: Molecular basis of $K^+$ conduction and selectivity*, Science, 280:69–77, 1998.
[7] W. Dyrka, M.M. Bartuzel, and M. Kotulska, *Optimization of 3D Poisson–Nernst–Planck model for fast evaluation of diverse protein channels*, Proteins Struct. Funct. Bioinforma., 81:1802–1822, 2013.
[8] B. Eisenberg, Y. Hyon, and C. Liu, *Energy variational analysis of ions in water and channels: Field theory for primitive models of complex ionic fluids*, J. Chem. Phys., 133:104104, 2010.
[9] B. Eisenberg and W. Liu, *Poisson–Nernst–Planck systems for ion channels with permanent charges*, SIAM J. Math. Anal., 38:1932–1966, 2007.

[10] B. Eisenberg and W. Nonner, *Shockley–Ramo theorem measures conformation changes of ion channels and proteins*, J. Comput. Electron., 6:363–365, 2007.
[11] D. Gillespie, W. Nonner, and R.S. Eisenberg, *Coupling Poisson–Nernst–Planck and density functional theory to calculate ion flux*, J. Phys. Condens. Matter, 14:12129–12145, 2002.
[12] Z. He, *Review of the Shockley–Ramo theorem and its application in semiconductor gamma-ray detectors*, Nucl. Instrum. Mech. A, 463:250–267, 2001.
[13] B. Hille et al., *Ion Channels of Excitable Membranes*, Sinauer Sunderland, MA, 2001.
[14] T.-L. Horng, T.-C. Lin, C. Liu, and B. Eisenberg, *PNP equations with steric effects: A model of ion flow through channels*, J. Phys. Chem. B, 116:11422–11441, 2012.
[15] Y. Hyon, B. Eisenberg, and C. Liu, *A mathematical model for the hard sphere repulsion in ionic solutions*, Commun. Math. Sci., 9:459–475, 2011.
[16] M. Ø. Jensen, V. Jogini, D.W. Borhani, A.E. Leffler, R.O. Dror, and D.E. Shaw, *Mechanism of voltage gating in potassium channels*, Science, 336:229–233, 2012.
[17] R.D. Keynes and E. Rojas, *Kinetics and steady-state properties of the charged system controlling sodium conductance in the squid giant axon*, J. Physiol., 239:393–434, 1974.
[18] J. Koch and F. von Oppen, *Franck–Condon blockade and giant Fano factors in transport through single molecules*, Phys. Rev. Lett., 94:206804, 2005.
[19] Y. Levin, *Electrostatic correlations: from plasma to biology*, Rep. Prog. Phys., 65(11):1577–1632, 2002.
[20] B. Lu and Y.C. Zhou, *Poisson–Nernst–Planck equations for simulating biomolecular diffusion-reaction processes II: Size effects on ionic distributions and diffusion-reaction rates*, Biophys. J., 100:2475–2485, 2011.
[21] G.S. Manning, *Limiting laws and counterion condensation in polyelectrolyte solutions I. Colligative properties*, J. Chem. Phys., 51(1):924-933, 1969.
[22] G.S. Manning, *The molecular theory of polyelectrolyte solutions with applications to the electrostatic properties of polynucleotides*, Q. Rev. Biophys., 11:179–246, 1978.
[23] E. Neher and B. Sakmann, *Single-channel currents recorded from membrane of denervated frog muscle fibres*, Nature, 260:799–802, 1976.
[24] K. Neyts, J. Beeckman, and F. Beunis, *Quasistationary current contributions in electronic devices*, Opto-Electronics Rev., 15:41–46, 2007.
[25] W. Nonner, A. Peyser, D. Gillespie, and B. Eisenberg, *Relating microscopic charge movement to macroscopic currents: the Ramo–Shockley theorem applied to ion channels*, Biophys. J., 87:3716–3722, 2004.
[26] B. Pellegrini, *Electric charge motion, induced current, energy balance, and noise*, Phys. Rev. B, 34:5921–5924, 1986.
[27] E. Perozo, R. MacKinnon, F. Bezanilla, and E. Stefani, *Gating currents from a nonconducting mutant reveal open-closed conformations in Shaker $K^+$ channels*, Neuron, 11:353–358, 1993.
[28] S. Ramo, *Currents induced by electron motion*, Proc. IRE, 27:584–585, 1939.
[29] D.C. Rees, G. Chang, and R.H. Spencer, *Crystallographic analyses of ion channels: Lessons and challenges*, J. Biol. Chem., 275:713–716, 2000.
[30] M.F. Schndeider and W.K. Chandler, *Voltage dependent charge movement in skeletal muscle: a possible step in excitation-contraction coupling*, Nature, 242:244–246, 1973.
[31] W. Shockley, *Currents to conductors induced by a moving point charge*, J. Appl. Phys., 9:635–636, 1938.
[32] A. Singer, D. Gillespie, J. Norbury, and R.S. Eisenberg, *Singular perturbation analysis of the steady-state Poisson–Nernst–Planck system: Applications to ion channels*, Eur. J. Appl. Math., 19:541–560, 2008.
[33] E. Stefani, L. Toro, E. Perozo, and F. Bezanilla, *Gating of Shaker $K^+$ channels: I. Ionic and gating currents*, Biophys. J., 66:996–1010, 1994.
[34] S. Talwar and J. W. Lynch, *Investigating ion channel conformational changes using voltage clamp fluorometry*, Neuropharmacology, 98:312, 2015.
[35] Z. Xu, M. Ma, and P. Liu, *Self-energy-modified Poisson–Nernst–Planck equations: WKB approximation and finite-difference approaches*, Phys. Rev. E, 90(1):013307–013307, 2014.
[36] P.D. Yoder, K. Gärtner, U. Krumbein, and W. Fichtner, *Optimized terminal current calculation for Monte Carlo device simulation*, IEEE T. Comput. Aid. D., 16:1082–1087, 1997.
[37] P.D. Yoder, K. Gartner, and W. Fichtner, *A generalized Ramo–Shockley theorem for classical to quantum transport at arbitrary frequencies*, J. Appl. Phys., 79:1951–1954, 1996.